

Modulating Metal–Organic Frameworks To Breathe: A Postsynthetic Covalent Modification Approach

Zhenqiang Wang and Seth M. Cohen*

Department of Chemistry and Biochemistry, University of California, San Diego, La Jolla, California 92093

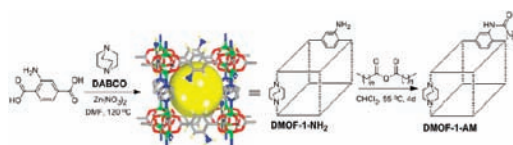
Received September 11, 2009; E-mail: scohen@ucsd.edu

Metal–organic frameworks (MOFs) represent a relatively new but increasingly important family of porous materials.¹ Because of their tunable structural features, high surface areas, and well-defined pore architectures, MOFs have found a wide variety of applications, including catalysis,^{2,3} gas storage,⁴ and separation.⁵ Whereas many MOFs are structurally rigid, a smaller group of MOF crystals show rather unique structural flexibility not commonly associated with crystalline solids.^{6–8} In particular, the guest-induced “gate opening”⁹ or “breathing”¹⁰ behaviors of MOFs, initially discovered by the groups of Kaneko,^{9,11} Kitagawa,^{12,13} Férey,^{10,14} and others,^{15–17} are currently under extensive investigation. These intriguing MOFs can selectively respond to certain guests and, upon gas/vapor adsorption, undergo reversible structural transitions between narrow pore (**np**) and large pore (**lp**) phases.⁸ Such a selective, stimuli-driven structural responsiveness is rarely observed in other classes of porous materials (e.g., zeolites, activated carbons, etc.) and therefore provides a unique entry into the development of functional materials for gas separation and sensing.¹⁸ These breathing processes can cause striking unit cell volume changes and frequently result in the appearance of steps and/or hysteresis behavior in their gas sorption isotherms. The breathing behavior in MOFs is best exemplified by MIL-53, where crystals of the MOF can sustain a cell shrinkage of up to 32% in volume upon hydration⁸ and where well-defined steps and hysteresis are apparent in the CO₂ sorption isotherms.¹⁹ On the basis of the analysis of sorption isotherms, powder X-ray diffraction (PXRD), and theoretical simulations, a better understanding of the breathing effects of MOFs has been achieved.^{20–23} A recent study has brought forth a thermodynamic description of the breathing behavior.^{24,25} However, from a synthetic standpoint, very few approaches or guidelines for modulating the flexibility of MOFs are available. Herein, we demonstrate, to the best of our knowledge, the first example of systematic modulation of the breathing effect in a MOF by chemical functionalization.²⁶ We show that a covalent postsynthetic modification (PSM) strategy can be used to modulate the breathing behavior of a MOF. Demonstrating that the breathing of a MOF can be altered by PSM has important implications for the use of these materials in gas storage, separation, and sensing.

Recently, several groups have demonstrated that targeting their organic components allows MOFs to be readily modified in a postsynthetic manner with a wide array of covalent transformations under mild conditions.^{27–29} In our previous studies, we showed that a number of amine-bearing MOFs, including IRMOF-3, UMCM-1-NH₂, and DMOF-1-NH₂, can be modified at the free amino groups with anhydrides and isocyanates.^{30–33} DMOF-1-NH₂ is an amino derivative of DMOF-1, a three-dimensional porous MOF constructed from Zn(II)-based paddle-wheel secondary building units, 1,4-benzenedicarboxylate, and pillaring 1,4-diazabicyclo[2.2.2]octane (DABCO) ligands (Scheme 1).³⁴ When treated with linear alkyl anhydrides (O[CO(CH₂)_nCH₃]₂, *n* = 0–5) in chloroform with gentle heating, DMOF-1-NH₂ can be readily converted to the corresponding amide

products, designated as DMOF-1-AM(*n*+1), with essentially complete conversion (>90%; Scheme 1 and Figure S1 in the Supporting Information). Notably, the modified MOFs retain their crystallinity and microporosity.³³

Scheme 1. Postsynthetic Modification of DMOF-1-NH₂ with Linear Alkyl Anhydrides



While examining the gas sorption properties of the modified DMOF samples, we discovered an unusual behavior. Modified MOFs with longer alkyl chains, such as DMOF-1-AM4, -AM5, and -AM6, exhibit reasonable porosity (based on N₂ sorption isotherms at 77 K; Figure S2), with calculated Brunauer–Emmett–Teller (BET) surface areas of ~700 m²/g (compared with ~1400 m²/g for unmodified DMOF-1-NH₂).³³ However, those with shorter alkyl chains, particularly DMOF-1-AM1 and -AM2, show unexpectedly low N₂ uptake at 77 K, giving rise to BET surface areas as low as ~300 m²/g (Figure S2). Since these DMOF-1-AM samples have similar percent conversions (Figure S1), these results are in drastic contrast to those seen in the IRMOF-3 system, in which the surface area of the modified MOFs is inversely proportional to the number of additional atoms as a result of PSM.³¹ Most interesting is DMOF-1-AM3, which at 77 K demonstrates a stepwise N₂ sorption profile, where the adsorption branch of the isotherm begins at relatively low uptake (<75 cm³/g STP), but starting at *P*/*P*₀ ≈ 0.015, the amount of adsorbed N₂ molecules sharply increases, reaching more than 100 cm³/g STP at *P*/*P*₀ = 0.020 (Figure 1). This abrupt transition amounts to an increase in surface area from ~316 to ~735 m²/g, as calculated by applying the BET equation to the adsorption data at *P*/*P*₀ = 0.001–0.014 and 0.03–0.13, respectively (Figure S3). It should also be noted that the desorption trace of the isotherm does not follow the adsorption branch, especially in the lower-pressure region, where the BET surface area is estimated to be ~797 m²/g using the desorption data at *P*/*P*₀ = 0.001–0.014 (Figure S4), thereby displaying a large hysteresis (the BET surface area is estimated to be ~763 m²/g using the desorption data at *P*/*P*₀ = 0.03–0.13). Finally, a much smaller hysteresis at higher partial pressures (*P*/*P*₀ > 0.4) is seen in both N₂ and Ar isotherms of all DMOF samples (including DMOF-1 and DMOF-1-NH₂). This minor hysteresis can be attributed to capillary condensation within mesoscale features,³⁵ which has been observed in other MOF systems and has been assigned to the presence of crystal defects.³⁶

The sorption behavior of DMOF-1-AM3 was further investigated using Ar at 87 K and CO₂ at 196 K within a pressure limit of *P* < 1.1 bar. While the Ar sorption profile at 87 K largely resembles that of N₂ at 77 K, only showing a slightly higher transition pressure

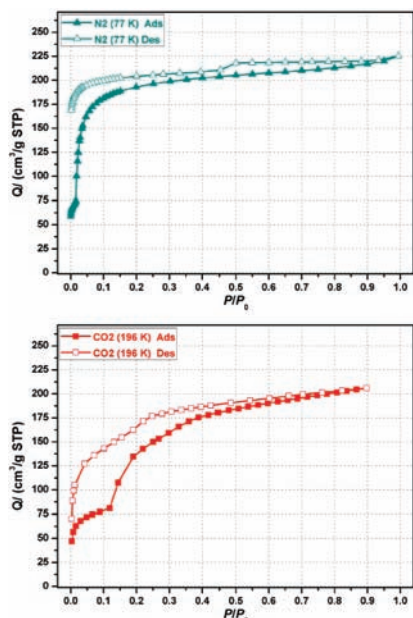


Figure 1. (top) N_2 sorption isotherm at 77 K and (bottom) CO_2 sorption isotherm at 196 K for DMOF-1-AM3.

($P/P_0 \approx 0.028$; Figure S5), the CO_2 isotherm at 196 K manifests much more pronounced steps and hysteresis, with a transition pressure ($P/P_0 \approx 0.12$) that is significantly higher than that for N_2 or Ar adsorption (Figure 1). Interestingly, other gas sorption isotherms involving H_2 at 77 K, CH_4 at 196 K, and CO_2 at higher temperatures (273, 296 K) do not display any well-defined steps or hysteresis (data not shown). Similar gas-specific isothermal sorption profiles have been observed for MIL-53 and are a strong indication of a breathing process featuring structural transitions between the **np** and **lp** forms.⁸

Gas sorption measurements with N_2 , Ar, and CO_2 were also obtained for DMOF-1- NH_2 and DMOF-1-AM1, -AM2, and -AM4. Unmodified DMOF-1- NH_2 clearly remains in the **lp** form and displays typical type-I sorption isotherms (Figure S6),³⁵ indicating no breathing in the parent material with any of the gases. This is consistent with the behavior of DMOF-1, which also primarily exists in the **lp** form (Figure S7),³⁴ with the exception of an isopropanol-induced multistep (**lp** \rightarrow **np** \rightarrow **lp**) transition.³⁷ With the shortest alkyl modification, DMOF-1-AM1 also shows essentially type-I isotherms for both N_2 and Ar uptake; however, with CO_2 , DMOF-1-AM1 begins to display nonideal type-I behavior and a small but unambiguous hysteresis (Figure S8). With DMOF-1-AM2, clear breathing behavior with all three gases is apparent (Figure S9); this is especially true with CO_2 at 196 K, for which a prominent step and large hysteresis are observed, similar to that seen with DMOF-1-AM3 (Figure 1). As already noted, DMOF-1-AM3 shows prototypical breathing behavior, but upon extension of the alkyl chain to give DMOF-1-AM4, the breathing behavior is not observed under these conditions, and type-I isotherms are found (Figure S10). These series of measurements show the gradual onset of breathing with increasing alkyl chain length up until DMOF-1-AM4, where breathing no longer occurs with the gases studied here.

The observed breathing behavior can satisfactorily account for the unusual difference in N_2 -measured surface areas between DMOF-1-AM1/-AM2 and DMOF-1-AM4/-AM5/-AM6 mentioned earlier. The observed N_2 -based porosity (Figure S2) is likely a reflection of the different phases in which these two groups of modified MOFs exist: while DMOF-1-AM4/-AM5/-AM6 are in the **lp** form (similar to unmodified DMOF-1- NH_2), DMOF-1-AM1/-

AM2 are in the **np** form, thereby showing an unexpectedly low surface area. DMOF-1-AM3, with an intermediate alkyl chain length, lies in the middle of these two groups and shows bistability with N_2 .

We propose that the low surface area of DMOF-1-AM1 and the distinct sorption behaviors of DMOF-1-AM2 and -AM3 originate from an enhanced stability of their **np** forms relative to their parent compounds (i.e., DMOF-1 and DMOF-1- NH_2) as a result of PSM. Indeed, while the **lp** phase of guest-free DMOF-1- NH_2 appears to be more stable than its **np** counterpart, this trend is reversed for DMOF-1-AM1, -AM2, and -AM3, giving rise to the **np** form in their guest-free phase. However, the difference in the relative stabilities of the two forms (**np** over **lp**) gradually diminishes as the length of alkyl chains increases, and for DMOF-1-AM4, the **lp** form is more stable. The overall effect of PSM in this system is that shorter alkyl chains favor the **np** structure (DMOF-1-AM1), longer alkyl chains stabilize the **lp** phase (DMOF-1-AM4, -AM5, -AM6), and the medium alkyl chains (DMOF-1-AM2, -AM3) lead to bistable formulations that can easily switch between the two forms, leading to the observed breathing. Sterics, weak chain-chain interactions, and/or chain flexibility may contribute to the observed dependence of breathing behavior on chain length.

To calculate the free-energy difference (ΔF_{host}) between the two guest-free forms, we applied the following modified equation, which can be derived from the thermodynamic model recently developed by Coudert et al.²⁴ by replacing the Langmuir equation with the Langmuir-Freundlich (LF) equation (Figure S11).³⁸

$$\Delta F_{\text{host}} = RT[n_2 N_{\text{max}}^2 \ln(1 + K_2 P_{\text{trans}}^{1/m_2}) - n_1 N_{\text{max}}^1 \ln(1 + K_1 P_{\text{trans}}^{1/m_1})]$$

Fitting both the adsorption and desorption branches of the CO_2 isotherm for DMOF-1-AM3 using the LF model (Figure 2) and applying the results to the above equation lead to an estimated ΔF_{host} value of 16–19 kJ/mol. The same calculation for DMOF-1-AM2 gives $\Delta F_{\text{host}} = 40$ –45 kJ/mol (Figure S12, Table S1). These results show that the difference in relative stability of the **np** and **lp** phases is smaller for DMOF-1-AM3, as observed experimentally. Additional evidence for the relative stability between the **np** and **lp** phases in these compounds is found in the PXRD patterns of guest-free DMOF samples. As shown in Figure 3, the two major peaks in DMOF-1- NH_2 , at $2\theta = \sim 8.0$ and 9.2° , are shifted to higher 2θ in DMOF-1-AM1 and -AM2, suggesting the increased stability of their corresponding **np** phase. DMOF-1-AM3 displays two sets of broader peaks that are attributable to the presence of both the **np** and **lp** phases, indicating its bistability (Figure 3).

Finally, it is instructive to compare the breathing behavior of DMOF-1-AM2 and -AM3 induced by CO_2 to that of DMOF-1 induced by isopropanol³⁷ and that of MIL-53 induced by CO_2 .¹⁹ Although these sorption isotherms share similar features, their breathing mechanisms are nevertheless fundamentally different. In the cases of DMOF-1 and MIL-53, the more favorable guest-free phase for both MOFs at ambient temperature is the **lp** form. Initial adsorption of isopropanol or CO_2 by the MOFs stabilizes the **np** form and facilitates the first structural transition (**lp** \rightarrow **np**), which is often not clearly observed since it typically occurs at extremely low pressures, where the adsorption isotherms of the two forms largely overlap.³⁹ Further adsorption of the guests, when it exceeds a certain value, begins to favor the **lp** form again and eventually leads to a second transition (**np** \rightarrow **lp**). The sorption profiles of these two MOF systems indeed exemplify “case c”, one of the four breathing cases proposed by Coudert et al.²⁴ In contrast, as a result of PSM, DMOF-1-AM2 and -AM3 start as **np** phases in their guest-

free forms. Uptake of CO₂ then stabilizes the **lp** form and thus induces the only structural transition (**np** → **lp**), which is reminiscent of what is described as “case a” by Coudert et al.²⁴

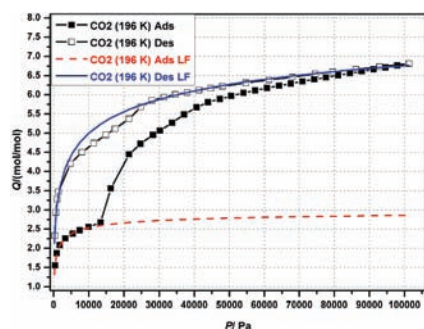


Figure 2. Langmuir–Freundlich (LF) fitting of the CO₂ sorption isotherm of DMOF-1-AM3 at 196 K.

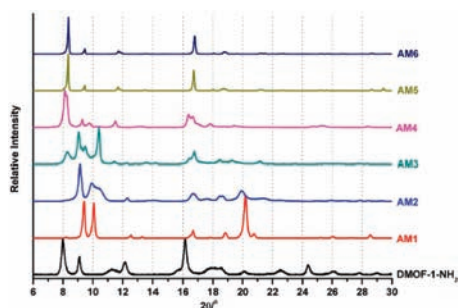


Figure 3. Powder X-ray diffraction (PXRD) patterns of dry DMOF-1-NH₂ and DMOF-1-AM1-6.

In summary, we have demonstrated that PSM can be used to modulate the breathing behavior in a MOF. These modified DMOF-1-AM materials provide a distinct platform for investigating the breathing effects found in only a handful of MOFs. The covalent attachment of appropriate organic functionalities to the MOF lattices considerably alters the relative stability of the **lp** and **np** phases, thereby making the materials either more or less prone to breathing. The ability to systematically tune the dynamic features of MOF structures, enabled by the covalent PSM approach, will eventually lead to the application of the modified materials in gas separation and sensing. Efforts to better understand the mechanism by which different substituents affect the relative stabilities of MOF structures are currently underway in our laboratory.

Acknowledgment. This work was supported by the University of California, San Diego, the National Science Foundation (CHE-0546531; instrumentation grants CHE-9709183, CHE-0116662, and CHE-0741968), and the Department of Energy (DE-FG02-08ER46519).

Supporting Information Available: Experimental details, Figures S1–S12, and Tables S1–S9. This material is available free of charge via the Internet at <http://pubs.acs.org>.

References

- (1) Long, J. R.; Yaghi, O. M. *Chem. Soc. Rev.* **2009**, *38*, 1213.
- (2) Ma, L. Q.; Abney, C.; Lin, W. B. *Chem. Soc. Rev.* **2009**, *38*, 1248.
- (3) Lee, J.; Farha, O. K.; Roberts, J.; Scheidt, K. A.; Nguyen, S. T.; Hupp, J. T. *Chem. Soc. Rev.* **2009**, *38*, 1450.
- (4) Murray, L. J.; Dinca, M.; Long, J. R. *Chem. Soc. Rev.* **2009**, *38*, 1294.
- (5) Li, J. R.; Kuppler, R. J.; Zhou, H. C. *Chem. Soc. Rev.* **2009**, *38*, 1477.
- (6) Kitagawa, S.; Uemura, K. *Chem. Soc. Rev.* **2005**, *34*, 109.
- (7) Halder, G. J.; Kepert, C. J. *Aust. J. Chem.* **2006**, *59*, 597.
- (8) Férey, G.; Serre, C. *Chem. Soc. Rev.* **2009**, *38*, 1380.
- (9) Li, D.; Kaneko, K. *Chem. Phys. Lett.* **2001**, *335*, 50.
- (10) Barthelet, K.; Marrot, J.; Riou, D.; Férey, G. *Angew. Chem., Int. Ed.* **2002**, *41*, 281.
- (11) Onishi, S.; Ohmori, T.; Ohkubo, T.; Noguchi, H.; Di, L.; Hanzawa, Y.; Kanoh, H.; Kaneko, K. *Appl. Surf. Sci.* **2002**, *196*, 81.
- (12) Uemura, K.; Kitagawa, S.; Kondo, M.; Fukui, K.; Kitaura, R.; Chang, H. C.; Mizutani, T. *Chem.–Eur. J.* **2002**, *8*, 3586.
- (13) Kitaura, R.; Fujimoto, K.; Noro, S.; Kondo, M.; Kitagawa, S. *Angew. Chem., Int. Ed.* **2002**, *41*, 133.
- (14) Serre, C.; Millange, F.; Thouvenot, C.; Noguès, M.; Marsolier, G.; Louër, D.; Férey, G. *J. Am. Chem. Soc.* **2002**, *124*, 13519.
- (15) Fletcher, A. J.; Cussen, E. J.; Prior, T. J.; Rosseinsky, M. J.; Kepert, C. J.; Thomas, K. M. *J. Am. Chem. Soc.* **2001**, *123*, 10001.
- (16) Cussen, E. J.; Claridge, J. B.; Rosseinsky, M. J.; Kepert, C. J. *J. Am. Chem. Soc.* **2002**, *124*, 9574.
- (17) Biradha, K.; Fujita, M. *Angew. Chem., Int. Ed.* **2002**, *41*, 3392.
- (18) Choi, H. S.; Suh, M. P. *Angew. Chem., Int. Ed.* **2009**, *48*, 6865.
- (19) Llewellyn, P. L.; Bourrelly, S.; Serre, C.; Filinchuk, Y.; Férey, G. *Angew. Chem., Int. Ed.* **2006**, *45*, 7751.
- (20) Ramsahye, N. A.; Maurin, G.; Bourrelly, S.; Llewellyn, P. L.; Loiseau, T.; Serre, C.; Férey, G. *Chem. Commun.* **2007**, 3261.
- (21) Serre, C.; Bourrelly, S.; Vimont, A.; Ramsahye, N. A.; Maurin, G.; Llewellyn, P. L.; Daturi, M.; Filinchuk, Y.; Leynaud, O.; Barnes, P.; Férey, G. *Adv. Mater.* **2007**, *19*, 2246.
- (22) Salles, F.; Ghoufi, A.; Maurin, G.; Bell, R. G.; Mellot-Draznieks, C.; Férey, G. *Angew. Chem., Int. Ed.* **2008**, *47*, 8487.
- (23) Llewellyn, P. L.; Maurin, G.; Devic, T.; Loera-Serna, S.; Rosenbach, N.; Serre, C.; Bourrelly, S.; Horcajada, P.; Filinchuk, Y.; Férey, G. *J. Am. Chem. Soc.* **2008**, *130*, 12808.
- (24) Coudert, F.-X.; Jeffroy, M.; Fuchs, A. H.; Boutin, A.; Mellot-Draznieks, C. *J. Am. Chem. Soc.* **2008**, *130*, 14294.
- (25) Coudert, F.-X.; Mellot-Draznieks, C.; Fuchs, A. H.; Boutin, A. *J. Am. Chem. Soc.* **2009**, *131*, 3442.
- (26) Couck, S.; Denayer, J. F. M.; Baron, G. V.; Rémy, T.; Gascon, J.; Kapteijn, F. *J. Am. Chem. Soc.* **2009**, *131*, 6326.
- (27) Kiang, Y. H.; Gardner, G. B.; Lee, S.; Xu, Z. T.; Lobkovsky, E. B. *J. Am. Chem. Soc.* **1999**, *121*, 8204.
- (28) Seo, J. S.; Whang, D.; Lee, H.; Jun, S. I.; Oh, J.; Jeon, Y. J.; Kim, K. *Nature* **2000**, *404*, 982.
- (29) Wang, Z.; Cohen, S. M. *Chem. Soc. Rev.* **2009**, *38*, 1315.
- (30) Wang, Z.; Cohen, S. M. *J. Am. Chem. Soc.* **2007**, *129*, 12368.
- (31) Tanabe, K. K.; Wang, Z.; Cohen, S. M. *J. Am. Chem. Soc.* **2008**, *130*, 8508.
- (32) Dugan, E.; Wang, Z.; Okamura, M.; Medina, A.; Cohen, S. M. *Chem. Commun.* **2008**, 3366.
- (33) Wang, Z.; Tanabe, K. K.; Cohen, S. M. *Inorg. Chem.* **2009**, *48*, 296.
- (34) Dybtsev, D. N.; Chun, H.; Kim, K. *Angew. Chem., Int. Ed.* **2004**, *43*, 5033.
- (35) Gregg, S. J.; Sing, K. S. W. *Adsorption, Surface Area, and Porosity*, 2nd ed.; Academic Press: London, 1982.
- (36) For examples, see: (a) Vishnyakov, A.; Ravikovitch, P. I.; Neimark, A. V.; Bulow, M.; Wang, Q. M. *Nano Lett.* **2003**, *3*, 713. (b) Lee, J.; Li, J.; Jagiello, J. *J. Solid State Chem.* **2005**, *178*, 2527. (c) Doonan, C. J.; Morris, W.; Furukawa, H.; Yaghi, O. M. *J. Am. Chem. Soc.* **2009**, *131*, 9492.
- (37) Uemura, K.; Yamasaki, Y.; Komagawa, Y.; Tanaka, K.; Kita, H. *Angew. Chem., Int. Ed.* **2007**, *46*, 6662.
- (38) In this equation, R is the gas constant, T is the temperature, P_{trans} is the transition pressure, and N_{max}^1 and N_{max}^2 are the saturation uptakes, K_1 and K_2 the binding constants, and n_1 and n_2 the coefficients for phases 1 and 2, respectively.
- (39) Boutin, A.; Springuel-Huet, M.-A.; Nossrov, A.; Gedeon, A.; Loiseau, T.; Volklinger, C.; Férey, G.; Coudert, F.-X.; Fuchs, A. H. *Angew. Chem., Int. Ed.* **2009**, *48*, 8314.

JA907742Z